iScience

CellPress
OPEN ACCESS

Article

Significant early end of the growing season of forest vegetation inside China's protected areas

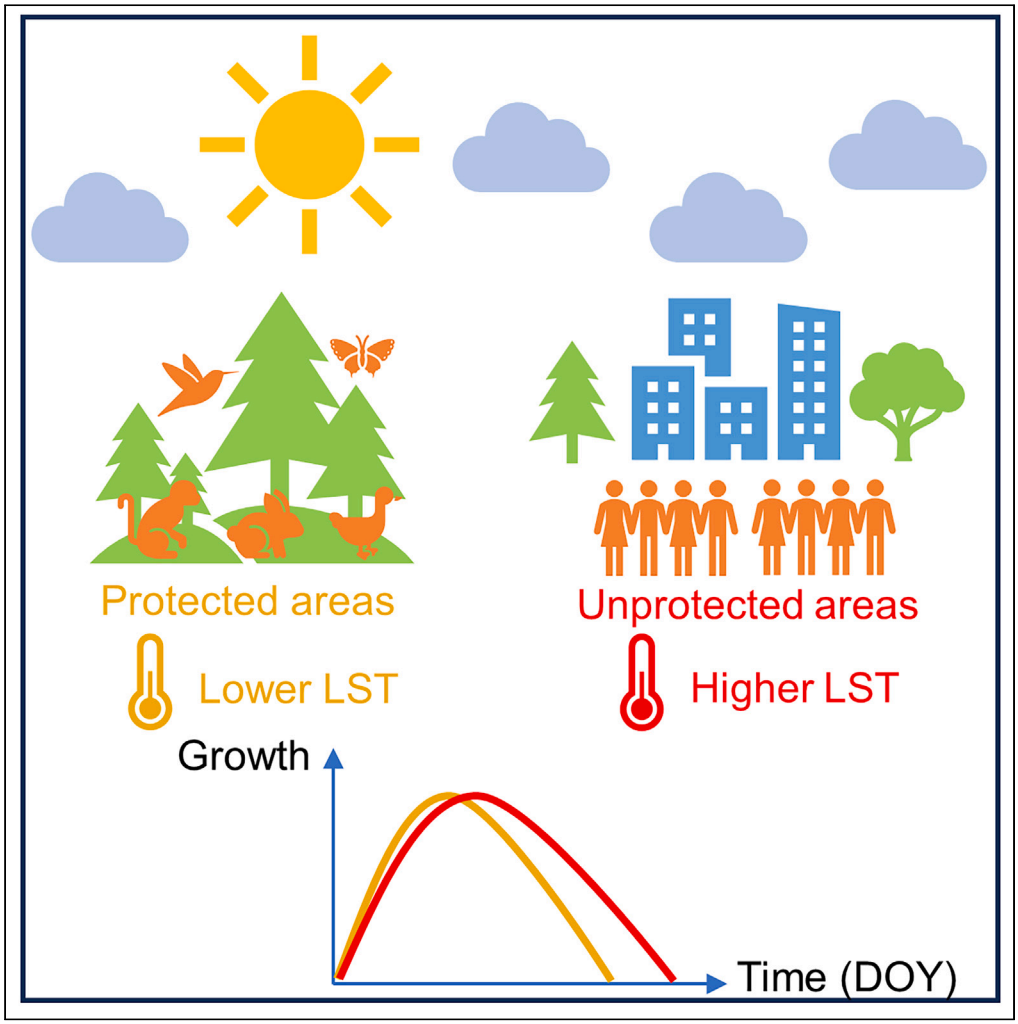

Ya Liu, Jun Ma

ma_jun@fudan.edu.cn

Highlights

Autumn forest phenology in China's protected areas (PAs) was earlier than outside

Phenological differences in and outside PAs increased in the last 20 years

Temperature differences inside and outside PAs caused phenological differences

Liu & Ma, iScience 27, 108652
January 19, 2024
https://doi.org/10.1016/j.isci.2023.108652

iScience

CellPress
OPEN ACCESS

Article

Significant early end of the growing season of forest vegetation inside China's protected areas

Ya Liu[1] and Jun Ma[1,2,*]

SUMMARY

The land surface phenology (LSP) indicators (i.e., start, end, and length of the growing season: SOS, EOS, LOS) are important to reflect the growth of forest and its response to environmental changes. However, the spatiotemporal variation and its mechanism of forest phenology under different human disturbance' levels are still unclear. Here, we compare the LSP indicators inside and outside China's 257 protected areas (PAs) and explore the influencing factors of phenological differences (ΔSOS, ΔEOS, ΔLOS). We find that in general, EOS inside PAs (mean ± s.e.m: 312.6 ± 1.2days) is significantly earlier than outside (314.6 ± 1.2days), and LOS inside PAs (218.9 ± 2.0days) are significantly shorter than outside (220.6 ± 2.0days). ΔSOS and ΔEOS are controlled by nighttime and daytime temperature differences, respectively, and both factors affect ΔLOS. This evidence provides a new understanding about the functions of PAs and its influence on forest vegetation growth.

INTRODUCTION

Forests play an irreplaceable role in regulating global carbon balance, mitigating climate change, and providing important ecosystem services for human survival and development.[1,2] The growing dynamics of forest vegetation are important for assessing the health of the forest ecosystems. In particular, as an important reflection of vegetation growth regular pattern and carbon sequestration, land surface vegetation phenology is a dynamic expression of the growth cycle of the forest and has been widely used in the study of forest-climate feedback.[3,4] Forest vegetation phenology is sensitive to changes in light, temperature, moisture, and other environmental factors, and vegetation phenological indexes have been widely used as sensitive indicators of climate change.[5–8] Therefore, how vegetation phenology responds to climatic conditions, under the context of global change, has become a hot issue in the field of global climate change and the carbon cycle in recent years.[9,10]

Many studies have shown that climate warming significantly affects both the spring and fall phenology of forest vegetation and alters the length of the growing season (LOS).[11–15] Especially, increasing attention has been focused on the impacts of human activities,[16] which are closely related to climatic conditions on vegetation phenology in recent years. Human activities cause changes in land cover and climate by altering the energy balance and material cycling, which in turn have had a significant impact on global forest vegetation phenology.[17,18] In the areas with intense human activities, the changes in forest vegetation phenology are more significant. For example, the heat island effect and CO_2 dome effect brought by urbanization significantly change vegetation phenology,[19] and the phenomenon of advanced greenup and delayed dormancy is more obvious in the areas near the cities.[20–22] It is noteworthy that with the widespread presence of human activities in natural ecosystems,[23,24] various degrees of human disturbance bring changes in environmental conditions for forest vegetation such as microclimate,[25,26] which have great impacts on vegetation phenology.[27,28] However, few studies have attempted to compare the spatiotemporal distribution of forest vegetation phenology characteristics under different levels of human disturbance and to investigate the mechanism behind such phenological differences.

Protected areas (PAs) are strictly conserved and have less human disturbance, compared to unprotected areas, due to the management policies. The strict management in PAs makes the abiotic environmental factors such as temperature and moisture significantly different from those outside and results in unique microclimate conditions,[29] which may have profound impacts on vegetation phenology and make PAs ideal "natural laboratories" for studies about the dynamics of vegetation growth and carbon sequestration and serving as an important reference under the scenario of human sustainable development. Considering that the degree of human disturbance is significantly different between protected areas and unprotected areas,[30,31] the differences in phenological indicators between these two types of areas can reflect the influence of the degree of disturbance on phenology. Previous studies have mostly focused on the dynamic changes of vegetation phenology,[32] feedback analysis of phenology on climate [33]and the regulatory effect of phenology on the ecosystem's carbon cycling[34] in

[1]Ministry of Education Key Laboratory for Biodiversity Science and Ecological Engineering, National Observations and Research Station for Wetland Ecosystems of the Yangtze Estuary, School of Life Sciences, Fudan University, #2005 Songhu Road, Shanghai 200438, China
[2]Lead contact
*Correspondence: ma_jun@fudan.edu.cn
https://doi.org/10.1016/j.isci.2023.108652

protected areas, but there is a lack of systematic evaluation and analysis on the impact of protected areas on vegetation phenology at a larger landscape scale. Other studies have focused on the impact of varying degrees of forest management on the temperature sensitivity of forest vegetation phenology,[35] and the phenological characteristics of economic crops.[36] However, there is a lack of in-depth and extensive exploration of the ecological mechanisms behind the impact of protected areas on vegetation phenology, such as how the differences in forest microclimate inside and outside protected areas further affect vegetation phenology. Especially, the differences in microclimatic conditions between inside and outside PAs vary with geographical locations, which limits the understanding of the complex relationship among human activity, climate change, and vegetation growth dynamics.

By 2020, China has established 10 types of PAs, which are widely distributed in various climate backgrounds, effectively protecting 90% of the country's terrestrial ecosystem types and covering 25% of the original natural forests.[37] Among them, the National Nature Reserve (NNR) with the largest number and area has the longest protection and management cycle and the most prominent value of protected objects.[38] Therefore, we take NNRs in China as the research objects here to explore the phenological indicators of forest vegetation and their influencing factors between inside and outside PAs. We used remote sensing datasets to extract the land surface phenology (LSP) indicators (i.e., start, end, and length of the growing season: SOS, EOS, LOS) and microclimatic indicators between inside and outside PAs. The objectives of this study were: (1) to explore the current differences in phenological indicators of the forest vegetation between inside and outside PAs and the relevant spatial variation (2018–2020) and temporal variation (2001–2020); (2) to detect the key factors affecting the phenological differences; and (3) to analyze the underlying mechanism of the spatiotemporal variation of these phenological differences between inside and outside of the PAs in China. The innovation of this study lies in the fact that for the first time, we constructed gradients within and outside protected areas on a national scale in China, and studied the phenological differences and driving factors between them, providing new insights into the current functions of protected areas in China.

RESULTS

Spatiotemporal variation of differences in phenological indicators between inside and outside PAs

There was no significant difference ($p > 0.05$) in the SOS between inside and outside PAs at the national scale and in each forest type (Table S2). However, at the national scale, EOS inside PAs (312.6 $\pm$ 1.2days) was significantly earlier ($p < 0.001$) than that outside PAs (314.6 $\pm$ 1.2days). Specifically for each forest type, EOS inside PAs of EBF (334.6 $\pm$ 2 days) was significantly earlier ($p < 0.05$) than that outside PAs (338.3 $\pm$ 1.8days), EOS inside PAs of DBF (302.6 $\pm$ 1.5 days) was significantly earlier ($p < 0.05$) than that outside PAs (303 $\pm$ 1.5 days), and EOS inside PAs of MF (310.9 $\pm$ 1.5 days) was significantly earlier ($p < 0.05$) than that outside PAs (313 $\pm$ 1.5 days), but there was no significant difference ($p > 0.05$) in the EOS between inside and outside PAs of ENF. Correspondingly, at the national scale, LOS inside PAs (218.9 $\pm$ 2.0days) was significantly shorter ($p < 0.001$) than that outside PAs (220.6 $\pm$ 2.0days). Specifically for each forest type, LOS inside PAs of EBF (254.1 $\pm$ 1.6 days) was significantly shorter ($p < 0.05$) than that outside PAs (256.3 $\pm$ 1.6days), LOS inside PAs of DBF (201.1 $\pm$ 3.2 days) was significantly shorter ($p < 0.05$) than that outside PAs (202 $\pm$ 3.5 days), and LOS inside PAs of MF (217 $\pm$ 2.7 days) was significantly shorter ($p < 0.05$) than that outside PAs (219.2 $\pm$ 2.7 days), but there was no significant difference ($p > 0.05$) in the LOS between inside and outside PAs of ENF.

Overall, about 53% of PAs have negative ΔSOS values, which were mainly distributed in Southwest and Southeast China (Figures 1A and 1D). While PAs with positive ΔSOS values (about 47%) were mainly distributed in Central and Northeast China. The lowest and the highest ΔSOS values reached −21days in Jianfengling Nature Reserve and 20days in Zhalong Nature Reserve, respectively. Besides, ΔEOS in 65% of PAs were negative (Figures 1B and 1E), and they were mainly distributed in Southeast, Southwest, and Northeast China with the lowest value of −27days in Wuliangshan Nature Reserve. While PAs with positive ΔEOS values (about 35%) were mainly distributed in South China, with the highest value of 13days in Cengwanglaoshan Nature Reserve. In addition, PAs of negative ΔLOS values (56%) were mainly located in Southwest, Northeast, and Central China with the lowest value of −27days in Zhalong Nature Reserve (Figures 1C and 1F). While PAs of positive ΔLOS values (44%) were mainly distributed in North China with the highest value of 21days in Zhumulangmafeng Nature Reserve.

In general, ΔSOS showed no trend with latitude gradient ($R^2 = 0.02$, $p > 0.05$), while ΔEOS increased ($R^2 = 0.22$, $p < 0.05$), which resulted in the upward trend of ΔLOS ($R^2 = 0.12$, $p < 0.05$) (Figures 1G–1I). Specifically, in the 20–25°N range, ΔSOS and ΔEOS showed a downward and upward trend, respectively (Figures 1G and 1H). While in the 25–35°N range, ΔSOS and ΔEOS both generally showed an upward consistent trend. In the 35–50°N range, ΔSOS fluctuated at the value of 0 with latitude gradient, while ΔEOS decreased at first and then sharply increased at about 48°N. In addition, ΔLOS showed a trend of increasing in the 20–40°N range and decreasing in the 35–50°N range but then increasing in the 50–52°N range (Figure 1I).

The interannual variation of phenological differences showed that the highest value of ΔSOS was 0.2 $\pm$ 0.4days in 2020, and the lowest was −1.2 $\pm$ 0.4days in 2005 (Figure 2A). The highest value of ΔEOS and ΔLOS were −1.5 $\pm$ 0.3days and −0.3 $\pm$ 0.5days in 2005, and the lowest was −2.7 $\pm$ 0.5days and −2.9 $\pm$ 0.6days in 2020 (Figures 2B and 2C). The Mann–Kendall test indicated that ΔSOS showed no trend ($z = 1.7$, $p > 0.05$) from 2001 to 2020, while ΔEOS and ΔLOS were both decreased (the statistic test outputs were both: $z = -2.4$, $p < 0.05$) with the change of years.

Specifically, for ΔSOS, there was no significant temporal trend in protected areas of each forest type (Figure S5A); For ΔEOS, PAs of MF ($z = -2.2$, $p < 0.05$) and DBF ($z = -2.1$, $p < 0.05$) showed a significant downward trend over time (Figure S5B); Similarly, for ΔLOS, only MF and DBF (the statistic test outputs were both: $z = -2.5$, $p < 0.05$) showed a significant downward trend over time (Figure S5C).

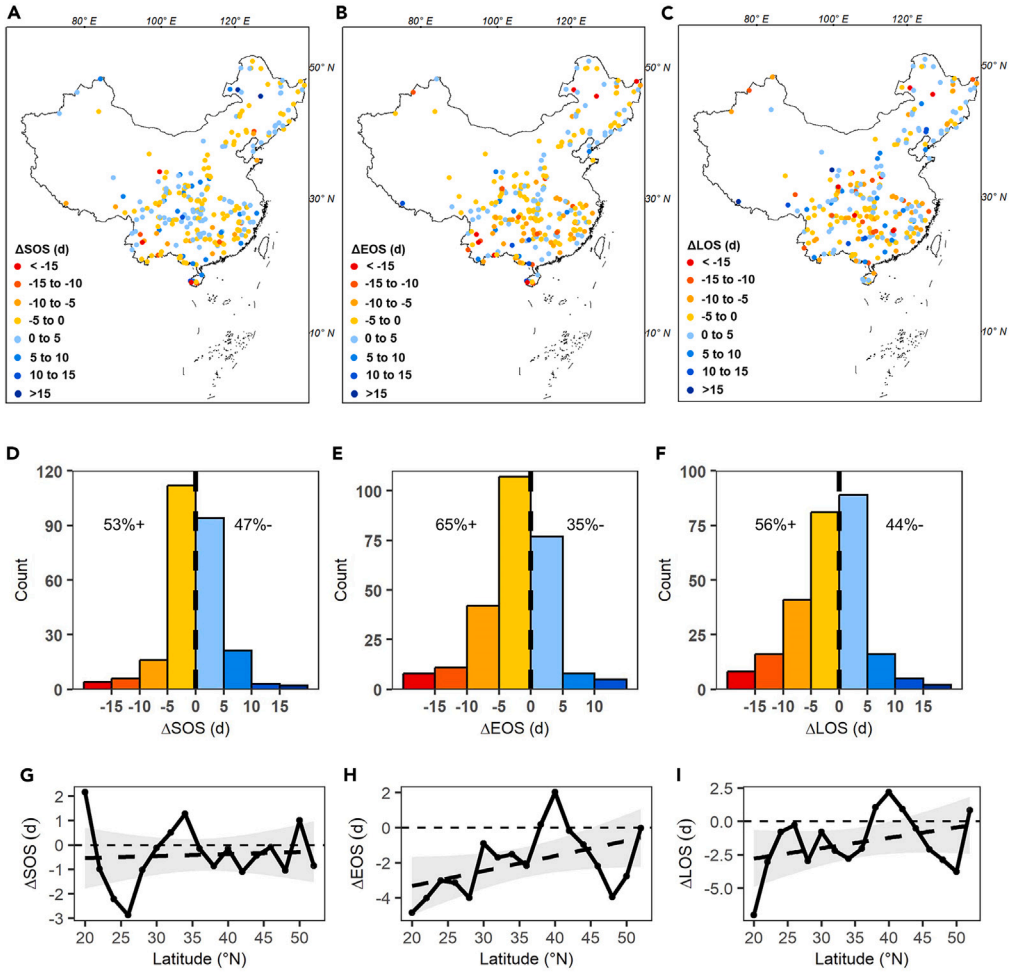

Figure 1. Spatial distributions of forest vegetation phenological differences between inside and outside protected areas (PAs)

(A–C) represents the overall distribution of ΔSOS, ΔEOS, and ΔLOS in the whole country respectively.

(D–F) represents the frequency distribution histogram of ΔSOS, ΔEOS, and ΔLOS.

(G–I) represents the line plot of the latitude distributions of ΔSOS, ΔEOS, and ΔLOS respectively, and the bolded dashed lines indicate linear regression fitting with the shaded areas representing 95% confidence intervals.

Drivers of phenological differences between inside and outside PAs

The partial correlation results showed that ΔSOS was only significantly related to ΔLST_night (partial correlation coefficient was −0.372, $p < 0.05$) (Figure 3A), and ΔEOS was only significantly related to ΔLST_day (partial correlation coefficient was 0.336, $p < 0.05$) (Figure 3B), while ΔLOS was both significantly related to ΔLST_day (partial correlation coefficient was 0.194, $p < 0.05$) and ΔLST_night (partial correlation coefficient was 0.303, $p < 0.05$) (Figure 3C).

For protected areas of each forest type, for PAs of MF, ΔSOS was only significantly related to ΔLST_night (partial correlation coefficient was −0.157, $p < 0.05$), and ΔEOS was only significantly related to ΔLST_day (partial correlation coefficient was 0.347, $p < 0.05$), while ΔLOS was both significantly related to ΔLST_day (partial correlation coefficient was 0.179, $p < 0.05$) and ΔLST_night (partial correlation coefficient was 0.324, $p < 0.05$) (Figures S6A–S6C). For PAs of ENF, there existed no significant relations between all phenological differences and variables. For PAs of EBF, ΔEOS and ΔLOS were only significantly related to ΔLST_day (partial correlation coefficient was 0.355 and 0.14, respectively, $p < 0.05$). For PAs of DBF, ΔSOS was only significantly related to ΔLST_night (partial correlation coefficient was −0.363, $p < 0.05$), and ΔEOS was only significantly related to ΔLST_day (partial correlation coefficient was 0.381, $p < 0.05$), while ΔLOS was both significantly related to ΔLST_day (partial correlation coefficient was 0.353, $p < 0.05$) and ΔLST_night (partial correlation coefficient was 0.245, $p < 0.05$) (Figures S6A–S6C).

Factors with significant influence are linearly fitted with ΔSOS, ΔEOS, and ΔLOS (Figure 4). The results showed that ΔSOS was significantly negatively correlated with ΔLST_night ($R^2 = 0.1$, $p < 0.001$), and ΔEOS was positively correlated with ΔLST_day ($R^2 = 0.13$, $p < 0.001$). In

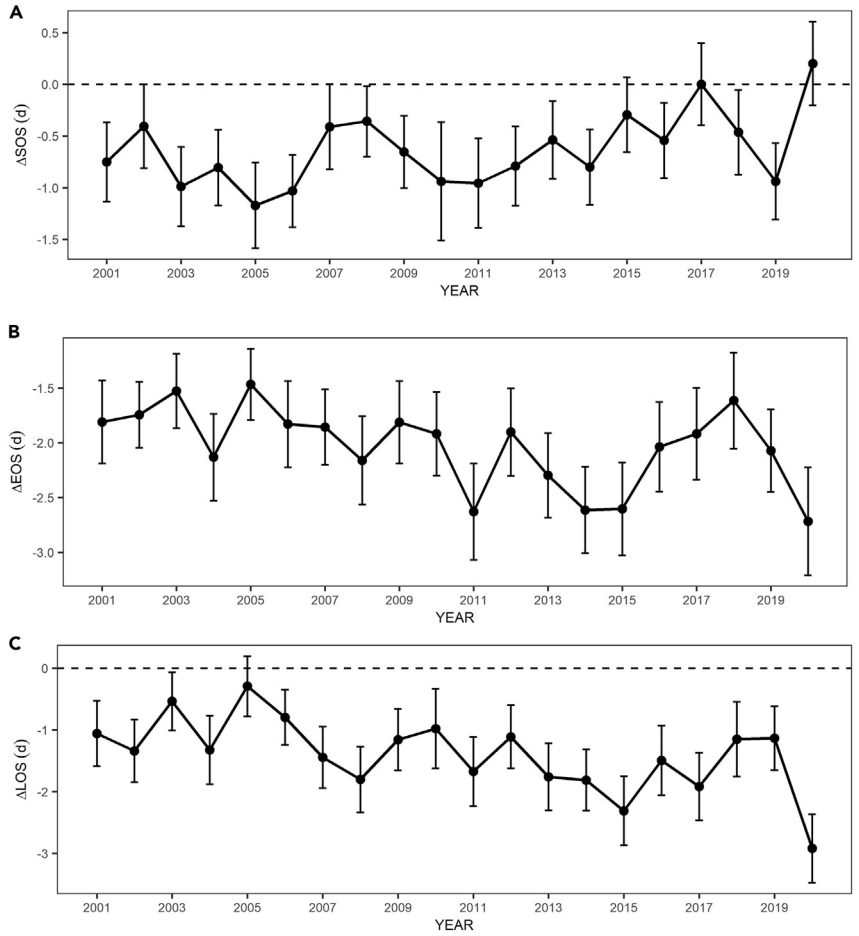

Figure 2. Annual variation of forest vegetation phenological differences between inside and outside protected areas (PAs) from 2001–2020

(A) ΔSOS; (B) ΔEOS; (C) ΔLOS. Scatter points represent mean values of phenological differences in each year, and error bars represent standard errors of the mean.

addition, ΔLST_day and ΔLST_night could independently explain 14% (R^2 = 0.14) and 11% (R^2 = 0.11) of the variation of ΔLOS, respectively, and it increased to 19% (R^2 = 0.19, $p < 0.001$) when the effects of ΔLST_day and ΔLST_night were considered together (Table S3).

DISCUSSION

Spatiotemporal variation of phenological differences between inside and outside PAs

Our research showed that there was a certain spatial heterogeneity of the phenological differences between inside and outside PAs both in spatial distribution and latitudinal gradient (Figure 1), and also indicated that PAs in China have the potential to advance the EOS and shorten the LOS of forest vegetation (Table S2). The advance of EOS means that forest vegetation enters the senescence stage earlier in protected areas, and the shortening of LOS means that the length of growing days for vegetation to conduct growth and development activities such as sprouting, spreading leaves is shorter in protected areas than outside.[4,39] Importantly, the differences (ΔEOS and ΔLOS) have gotten greater over the past 20 years (Figure 2). It is likely that the longer the PAs functions, the greater the differences of environmental factors such as microclimatic conditions inside and outside PAs become, which in turn leads to the interannual trends in phenological differences.

Specifically, only the phenological differences of PAs of ENF were not significant (Table S2). These PAs only account for 5% of the total protected areas and are mainly distributed in the southwest of China and the southeastern edge of the Qinghai Tibet Plateau, (Figure S3) where human activities are relatively low due to high altitude and harsh climate,[40,41] and the microclimate differences inside and outside these protected areas are not as significant as other types (Table S2).

In contrast, PAs of DBF and MF are widely distributed in Central, Southern, and Northeast China (Figure S3), where the population density and human disturbance are relatively high. The impact of protected areas is strong in this area, so the phenological differences increase with years (Figures S5B and S5C). In addition, the phenological differences at PAs of EBF are relatively stable and have maintained a relatively high impact in the past 20 years (Figures S5A–S5C).

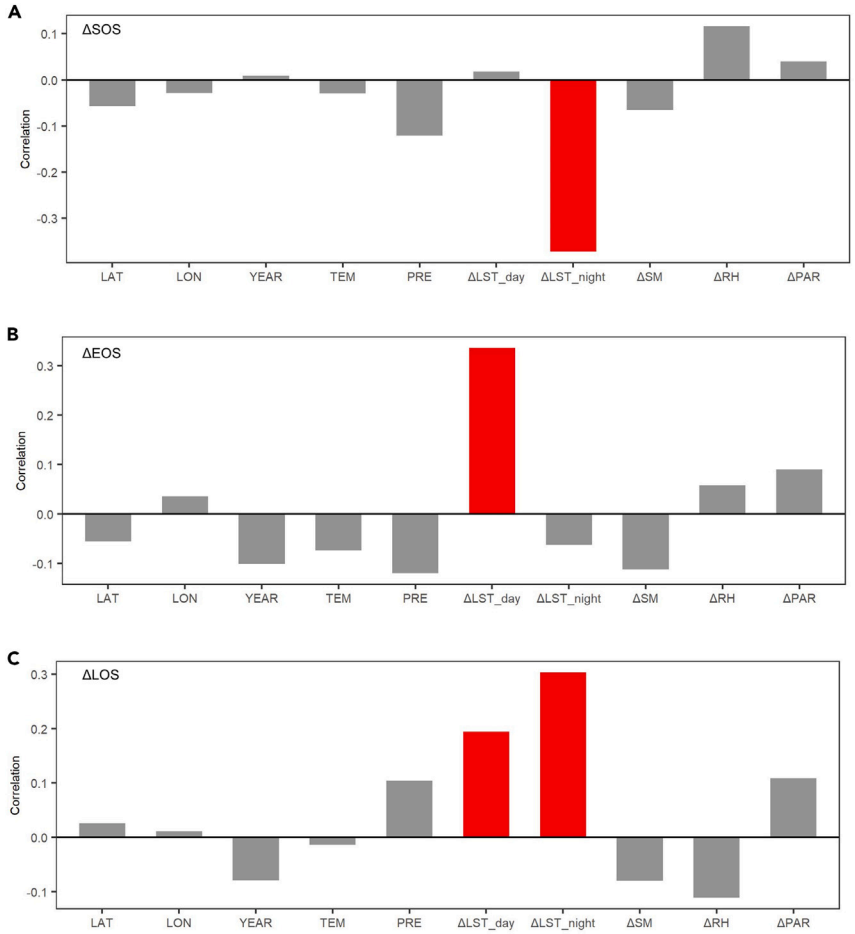

Figure 3. Controlling factors of phenological differences between inside and outside PAs

(A) ΔSOS; (B) ΔEOS; (C) ΔLOS. The factors are: LAT, latitude; LON, longitude; YEAR, the year in which the PA was established; TEM, mean annual air temperature; PRE, mean annual precipitation; ΔLST_day, daytime LST difference; ΔLST_night, nighttime LST difference; ΔSM, soil moisture difference; ΔRH, relative humidity difference; ΔPAR, photosynthetically active radiation difference. The red columns indicate significant variables ($p < 0.05$), while the gray columns indicate insignificant variables ($p > 0.05$).

The mechanism of climatic factors affecting phenological differences

As "natural laboratories" without human disturbance under ideal conditions, PAs can provide a more primitive and stable growth environment with less land cover change. Compared with outside unprotected areas which are frequently disturbed or converted to various land types, PAs usually have higher forest vegetation coverage, thus effectively reducing surface temperature.[42] On the other hand, there is a relatively higher intensity of human disturbance outside PAs, and the decrease of forest surface soil coverage with the corresponding increase of soil evaporation leads to a relatively higher surface temperature.[43,44] In our study, this is mainly reflected in the cooling effect of PAs on the highest daily temperature (Table S2).

Our results showed that the SOS differences between inside and outside PAs were negatively related to the nighttime temperature differences between inside and outside PAs, and the EOS differences were positively related to daytime temperature differences. This means that the larger differences in nighttime temperature led to smaller SOS differences (Figures 3A and 4A), and the larger differences in daytime temperature led to greater EOS differences (Figures 3B and 4B). As a result, the larger the differences in daytime temperature differences and nighttime temperature differences, the larger the length of the growing season (Figures 3C, 4C, and 4D; Table S3).

The driving factors for phenological differences in different forest types of PAs also varied. Among them, the driving factors of the phenological differences at PAs of MF and DBF were consistent with the national scale (Figure S6), the phenological differences at PAs of ENF were not related to microclimate differences, and EOS differences and LOS differences at PAs of EBF were related to LST_ Day differences (Figures S6B and S6C). The possible reason is that ENF is a special type of regional vegetation that has adapted to the alpine climate, and its phenology may also be affected by some local factors such as mowing and grazing under the forest.[45] In addition, the pattern of phenological differences' drivers at PAs of EBF showed the importance of daily highest temperature, which is a direct factor affecting vegetation photosynthesis and growth season[46] (Figure S6).

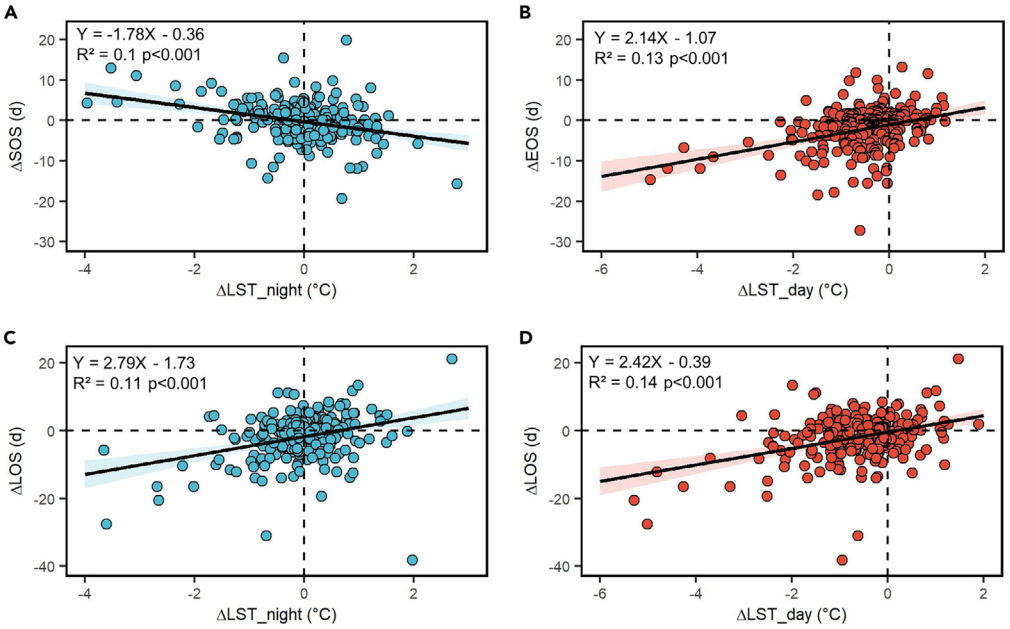

Figure 4. Linear regression fitting graph between phenological differences and major controlling variables

(A)ΔSOS∼ΔLST_night; (B)ΔEOS∼ΔLST_day; (C) ΔLOS∼ΔLST_night; (D) ΔLOS∼ΔLST_day. The solid lines indicate significant trends and the shaded areas represent 95% confidence intervals.

Consistent with previous studies, our research also showed that temperature is the most important factor regulating forest vegetation phenology.[3,47] For example, temperature is generally regarded as the main factor affecting SOS, which can influence phenology by regulating the chilling accumulation and heat requirement of vegetation.[48] At the same time, there is also some evidence that temperature has an impact on autumn phenology,[49,50] especially the asymmetry between daytime temperature and nighttime temperature effects.[46] This also indicates the necessity of distinguishing between the two temperatures here.

In summary, the results above confirm the claims proposed in some studies that microclimate has a regulatory effect on forest vegetation phenology.[27,28] It is worth noting that the forest vegetation phenology affected by microclimate can in turn regulate the microclimate condition.[3] For example, the variations of phenology that closely reflect the growth status of forest vegetation can also contribute to the variations in microclimates such as temperature,[51] and water conditions.[52] Therefore, the correlation revealed in this study cannot be simply regarded as a causal relationship, as it is not a one-way mechanism.

Ecological insights

The autumn phenology of forest vegetation has important ecological and evolutionary significance and is also an important component of the impact of climate change on ecosystems.[53] The process of leaf senescence is triggered by the accumulation of abscisic acid[54] with degradation of chlorophyll levels and other pigments (for example, beta carotene and lutein) and remobilization of nutrients.[55]

The phenomenon of earlier EOS and shorter LOS in the protected area may be an adaptation of forests to low temperatures, ending the growing season as early as possible to prevent frostbite in winter, which has a greater negative impact on vegetation productivity than the shortening of the growth season length.[56,57] Despite there is growing evidence that the autumn phenology of forest vegetation plays a critical role in regulating the length of the growing season and therefore the interannual variability of carbon uptake,[58,59] the rate of soil carbon decomposition will also decrease under lower temperature conditions in PAs, so shortening the length of the growth season does not necessarily reduce the net carbon uptake of forest ecosystems inside protected area.[60]

The novelty of this study is that we established the gradient inside and outside the PAs, and studied the phenological differences between them and the reasons for such differences. The areas inside and outside PAs in this study were considered to have different levels of human disturbance, and to some extent, they represented two different stages of forest protection. Therefore, the forest vegetation phenology in PAs can be used as a reference for the future status of many unprotected areas, which is crucial for us to address local forest management and planning. With the rapid development of geographic informatics and vegetation phenology in recent years, we look forward to a more comprehensive and robust assessment of the impact of protected areas on forest vegetation phenology in the world in the future.

Limitations of the study

It is important to note that there still are some uncertainties in our analysis. This study focuses on the phenological differences of forest vegetation under different human disturbance conditions. However, it is inevitable that although we strictly control the consistency of climate and

social environmental conditions inside and outside the protected areas pixels for comparison, some uncontrollable natural factors (such as forest wildfire,[10] forest diseases caused by pests,[61] etc.) may also interfere with our assessment of the effect of protected areas. The focus of future research should be on developing more rigorous methods for evaluating the benefits of protected areas to minimize the interference of these natural factors. In addition, remote sensing products based on vegetation index may contain some noise signals from the soil background,[62,63] such as soil color, artificial green buildings, and other non-photosynthetic materials. Although the phenological study based on satellite remote sensing datasets is an important reference for understanding the response of vegetation to global climate change, it cannot completely replace direct observation in-ground sites. In addition, due to the lack of extensive ground phenological sites in China, we cannot verify our conclusions using ground data for the time being.

STAR★METHODS

Detailed methods are provided in the online version of this paper and include the following:

- KEY RESOURCES TABLE
- RESOURCE AVAILABILITY
  - Lead contact
  - Materials availability
  - Data and code availability
- METHOD DETAILS
  - Selection of PAs
  - PAs' inside and outside gradients
  - Extraction of LSP indicators
  - Climatic data
  - Quantifying differences in indicators inside and outside protected areas
  - Classification of protected areas
- QUANTIFICATION AND STATISTICAL ANALYSIS

SUPPLEMENTAL INFORMATION

Supplemental information can be found online at https://doi.org/10.1016/j.isci.2023.108652.

ACKNOWLEDGMENTS

This research was supported by the Natural Science Foundation of China [grant number 32271659 and U2106209]; the Scientific Research Program of Shanghai Science and Technology Commission [grant number 21ZR1405600, 20dz1204702, and 23DZ1204504].

AUTHOR CONTRIBUTIONS

J.M. conceived the ideas and designed the methodology; Y.L. collected, analyzed the data, and wrote the manuscript. All authors contributed critically to the drafts and gave final approval for publication.

DECLARATION OF INTERESTS

The authors declare no competing interests.

Received: August 14, 2023
Revised: September 18, 2023
Accepted: December 4, 2023
Published: December 7, 2023

REFERENCES

1. Pugh, T.A.M., Lindeskog, M., Smith, B., Poulter, B., Arneth, A., Haverd, V., and Calle, L. (2019). Role of forest regrowth in global carbon sink dynamics. Proc. Natl. Acad. Sci. USA *116*, 4382–4387.
2. Jiang, M., Medlyn, B.E., Drake, J.E., Duursma, R.A., Anderson, I.C., Barton, C.V.M., Boer, M.M., Carrillo, Y., Castañeda-Gómez, L., Collins, L., et al. (2020). The fate of carbon in a mature forest under carbon dioxide enrichment. Nature *580*, 227–231.
3. Piao, S., Liu, Q., Chen, A., Janssens, I.A., Fu, Y., Dai, J., Liu, L., Lian, X., Shen, M., and Zhu, X. (2019). Plant phenology and global climate change: Current progresses and challenges. Glob. Chang. Biol. *25*, 1922–1940.
4. Berra, E.F., and Gaulton, R. (2021). Remote sensing of temperate and boreal forest phenology: A review of progress, challenges and opportunities in the intercomparison of in-situ and satellite phenological metrics. For. Ecol. Manage. *480*, 118663.
5. Richardson, A.D., Keenan, T.F., Migliavacca, M., Ryu, Y., Sonnentag, O., and Toomey, M. (2013). Climate change, phenology, and phenological control of vegetation feedbacks to the climate system. Agric. For. Meteorol. *169*, 156–173.
6. Körner, C., and Basler, D. (2010). Phenology Under Global Warming. Science *327*, 1461–1462.
7. Fu, Y.H., Zhang, X., Piao, S., Hao, F., Geng, X., Vitasse, Y., Zohner, C., Peñuelas, J., and Janssens, I.A. (2019). Daylength helps

temperate deciduous trees to leaf-out at the optimal time. Glob. Chang. Biol. *25*, 2410–2418.
8. Peaucelle, M., Janssens, I.A., Stocker, B.D., Descals Ferrando, A., Fu, Y.H., Molowny-Horas, R., Ciais, P., and Peñuelas, J. (2019). Spatial variance of spring phenology in temperate deciduous forests is constrained by background climatic conditions. Nat. Commun. *10*, 5388.
9. Arora, V.K., and Boer, G.J. (2010). Uncertainties in the 20th century carbon budget associated with land use change. Glob. Chang. Biol. *16*, 3327–3348.
10. Curtis, P.G., Slay, C.M., Harris, N.L., Tyukavina, A., and Hansen, M.C. (2018). Classifying drivers of global forest loss. Science *361*, 1108–1111.
11. Xie, J., Hüsler, F., de Jong, R., Chimani, B., Asam, S., Sun, Y., Schaepman, M.E., and Kneubühler, M. (2021). Spring Temperature and Snow Cover Climatology Drive the Advanced Springtime Phenology (1991-2014) in the European Alps. JGR. Biogeosciences *126*. e2020JG006150.
12. Ge, Q., Wang, H., Rutishauser, T., and Dai, J. (2015). Phenological response to climate change in China: a meta-analysis. Glob. Chang. Biol. *21*, 265–274.
13. Li, C., Wang, R., Cui, X., Wu, F., Yan, Y., Peng, Q., Qian, Z., and Xu, Y. (2021). Responses of vegetation spring phenology to climatic factors in Xinjiang. Ecol. Indic. *124*, 107286.
14. Liu, Q., Fu, Y.H., Zhu, Z., Liu, Y., Liu, Z., Huang, M., Janssens, I.A., and Piao, S. (2016). Delayed autumn phenology in the Northern Hemisphere is related to change in both climate and spring phenology. Glob. Chang. Biol. *22*, 3702–3711.
15. Fu, Y.H., Piao, S., Op de Beeck, M., Cong, N., Zhao, H., Zhang, Y., Menzel, A., and Janssens, I.A. (2014). Recent spring phenology shifts in western Central Europe based on multiscale observations. Glob. Ecol. Biogeogr. *23*, 1255–1263.
16. Qu, S., Wang, L., Lin, A., Yu, D., Yuan, M., and Li, C. (2020). Distinguishing the impacts of climate change and anthropogenic factors on vegetation dynamics in the Yangtze River Basin, China. Ecol. Indic. *108*, 105724. Unsp 105724.
17. Buitenwerf, R., Sandel, B., Normand, S., Mimet, A., and Svenning, J.C. (2018). Land surface greening suggests vigorous woody regrowth throughout European semi-natural vegetation. Glob. Chang. Biol. *24*, 5789–5801.
18. Watson, J.E.M., Evans, T., Venter, O., Williams, B., Tulloch, A., Stewart, C., Thompson, I., Ray, J.C., Murray, K., Salazar, A., et al. (2018). The exceptional value of intact forest ecosystems. Nat. Ecol. Evol. *2*, 599–610.
19. Wang, S., Ju, W., Peñuelas, J., Cescatti, A., Zhou, Y., Fu, Y., Huete, A., Liu, M., and Zhang, Y. (2019). Urban-rural gradients reveal joint control of elevated CO2 and temperature on extended photosynthetic seasons. Nat. Ecol. Evol. *3*, 1076–1085.
20. Kabano, P., Lindley, S., and Harris, A. (2021). Evidence of urban heat island impacts on the vegetation growing season length in a tropical city. Landsc. Urban Plan. *206*, 103989.
21. Jia, W., Zhao, S., Zhang, X., Liu, S., Henebry, G.M., and Liu, L. (2021). Urbanization imprint on land surface phenology: The urban-rural gradient analysis for Chinese cities. Glob. Chang. Biol. *27*, 2895–2904.
22. Zhang, X., Friedl, M.A., Schaaf, C.B., Strahler, A.H., and Schneider, A. (2004). The footprint of urban climates on vegetation phenology. Geophys. Res. Lett. *31*, L12209.
23. Marques, A., Martins, I.S., Kastner, T., Plutzar, C., Theurl, M.C., Eisenmenger, N., Huijbregts, M.A.J., Wood, R., Stadler, K., Bruckner, M., et al. (2019). Increasing impacts of land use on biodiversity and carbon sequestration driven by population and economic growth. Nat. Ecol. Evol. *3*, 628–637.
24. Singh, S.P. (1998). Chronic disturbance, a principal cause of environmental degradation in developing countries. Environ. Conserv. *25*, 1–2.
25. Vlassova, L., and Pérez-Cabello, F. (2016). Effects of post-fire wood management strategies on vegetation recovery and land surface temperature (LST) estimated from Landsat images. Int. J. Appl. Earth Obs. Geoinf. *44*, 171–183.
26. Jean, M., Alexander, H.D., Mack, M.C., and Johnstone, J.F. (2017). Patterns of bryophyte succession in a 160-year chronosequence in deciduous and coniferous forests of boreal Alaska. Can. J. For. Res. *47*, 1021–1032.
27. Hwang, T., Song, C., Vose, J.M., and Band, L.E. (2011). Topography-mediated controls on local vegetation phenology estimated from MODIS vegetation index. Landsc. Ecol. *26*, 541–556.
28. Ward, S.E., Schulze, M., and Roy, B. (2018). A long-term perspective on microclimate and spring plant phenology in the Western Cascades. Ecosphere *9*, e02451.
29. Thom, D., Sommerfeld, A., Sebald, J., Hagge, J., Müller, J., and Seidl, R. (2020). Effects of disturbance patterns and deadwood on the microclimate in European beech forests. Agric. For. Meteorol. *291*, 108066.
30. Gray, C.L., Hill, S.L.L., Newbold, T., Hudson, L.N., Börger, L., Contu, S., Hoskins, A.J., Ferrier, S., Purvis, A., and Scharlemann, J.P.W. (2016). Local biodiversity is higher inside than outside terrestrial protected areas worldwide. Nat. Commun. *7*, 12306.
31. Freudenberger, L., Hobson, P.R., Rupic, S., Pe'er, G., Schluck, M., Sauermann, J., Kreft, S., Selva, N., and Ibisch, P.L. (2013). Spatial road disturbance index (SPROADI) for conservation planning: a novel landscape index, demonstrated for the State of Brandenburg, Germany. Landsc. Ecol. *28*, 1353–1369.
32. Lara, C., Saldías, G.S., Cazelles, B., Rivadeneira, M.M., Muñoz, R., Galán, A., Paredes, Á.L., Fierro, P., and Broitman, B.R. (2021). Climatic Regulation of Vegetation Phenology in Protected Areas along Western South America. Remote Sens *13*, 2590.
33. O'Leary, D.S., Kellermann, J.L., and Wayne, C. (2018). Snowmelt timing, phenology, and growing season length in conifer forests of Crater Lake National Park, USA. Int. J. Biometeorol. *62*, 273–285.
34. Li, B., Huang, F., Qin, L., Qi, H., and Sun, N. (2019). Spatio-Temporal Variations of Carbon Use Efficiency in Natural Terrestrial Ecosystems and the Relationship with Climatic Factors in the Songnen Plain, China. Remote Sens *11*, 2513.
35. Ma, J., Xiao, X., Li, R., Zhao, B., and Myint, S.W. (2020). Enhanced spring phenological temperature sensitivity explains the extension of carbon uptake period in temperate forest protected areas. For. Ecol. Manage. *455*, 117679.
36. de Alcântara, M.S., Duarte, A.E., Boligon, A.A., de Campos, M.M.A., de Lucena, R.F.P., Pinheiro, M.A., and da Cruz, D.D. (2020). Effects of different levels of exploration on the ecological processes of Dimorphandra gardneriana, a tropical savanna tree. Environ. Monit. Assess. *192*, 378.
37. State Forestry Administration (2020). China Nature Reserve.
38. Li, B.V., and Pimm, S.L. (2020). How China expanded its protected areas to conserve biodiversity. Curr. Biol. *30*, R1334–R1340.
39. Caparros-Santiago, J.A., Rodriguez-Galiano, V., and Dash, J. (2021). Land surface phenology as indicator of global terrestrial ecosystem dynamics: A systematic review. ISPRS J. Photogramm. Remote Sens. *171*, 330–347.
40. Cetin, M. (2020). Climate comfort depending on different altitudes and land use in the urban areas in Kahramanmaras City. Air Qual. Atmos. Health *13*, 991–999.
41. Liu, J., Xin, Z., Huang, Y., and Yu, J. (2022). Climate suitability assessment on the Qinghai-Tibet Plateau. Sci. Total Environ. *816*, 151653.
42. Xu, X., Huang, A., Belle, E., De Frenne, P., and Jia, G. (2022). Protected areas provide thermal buffer against climate change. Sci. Adv. *8*, eabo0119.
43. Hirsch, A.L., Pitman, A.J., and Kala, J. (2014). The role of land cover change inmodulating the soil moisture-temperature land-atmosphere coupling strength over Australia. Geophys. Res. Lett. *41*, 5883–5890.
44. Jiang, Y., Fu, P., and Weng, Q. (2015). Assessing the Impacts of Urbanization-Associated Land Use/Cover Change on Land Surface Temperature and Surface Moisture: A Case Study in the Midwestern United States. Remote Sens *7*, 4880–4898.
45. Shen, M., Wang, S., Jiang, N., Sun, J., Cao, R., Ling, X., Fang, B., Zhang, L., Zhang, L., Xu, X., et al. (2022). Plant phenology changes and drivers on the Qinghai-Tibetan Plateau. Nat. Rev. Earth Environ. *3*, 633–651.
46. Wu, C., Wang, X., Wang, H., Ciais, P., Peñuelas, J., Myneni, R.B., Desai, A.R., Gough, C.M., Gonsamo, A., Black, A.T., et al. (2018). Contrasting responses of autumn-leaf senescence to daytime and night-time warming. Nat. Clim. Chang. *8*, 1092–1096.
47. Du, J., He, Z., Piatek, K.B., Chen, L., Lin, P., and Zhu, X. (2019). Interacting effects of temperature and precipitation on climatic sensitivity of spring vegetation green-up in arid mountains of China. Agric. For. Meteorol. *269–270*, 71–77.
48. Wang, H., Wu, C., Ciais, P., Peñuelas, J., Dai, J., Fu, Y., and Ge, Q. (2020). Overestimation of the effect of climatic warming on spring phenology due to misrepresentation of chilling. Nat. Commun. *11*, 4945.
49. Zhu, W., Tian, H., Xu, X., Pan, Y., Chen, G., and Lin, W. (2012). Extension of the growing season due to delayed autumn over mid and high latitudes in North America during 1982-2006. Glob. Ecol. Biogeogr. *21*, 260–271.
50. Barichivich, J., Briffa, K.R., Myneni, R.B., Osborn, T.J., Melvin, T.M., Ciais, P., Piao, S., and Tucker, C. (2013). Large-scale variations in the vegetation growing season and annual cycle of atmospheric CO2 at high northern latitudes from 1950 to 2011. Glob. Chang. Biol. *19*, 3167–3183.
51. Loranty, M.M., Berner, L.T., Goetz, S.J., Jin, Y., and Randerson, J.T. (2014). Vegetation controls on northern high latitude snow-albedo feedback: observations and CMIP5 model simulations. Glob. Chang. Biol. *20*, 594–606.
52. Kim, J.H., Hwang, T., Yang, Y., Schaaf, C.L., Boose, E., and Munger, J.W. (2018).

Warming-Induced Earlier Greenup Leads to Reduced Stream Discharge in a Temperate Mixed Forest Catchment. JGR. Biogeosciences *123*, 1960–1975.
53. Wu, C., Peng, J., Ciais, P., Peñuelas, J., Wang, H., Beguería, S., Andrew Black, T., Jassal, R.S., Zhang, X., Yuan, W., et al. (2022). Increased drought effects on the phenology of autumn leaf senescence. Nat. Clim. Chang. *12*, 943–949.
54. Zhao, Y., Chan, Z., Gao, J., Xing, L., Cao, M., Yu, C., Hu, Y., You, J., Shi, H., Zhu, Y., et al. (2016). ABA receptor PYL9 promotes drought resistance and leaf senescence. Proc. Natl. Acad. Sci. USA *113*, 1949–1954.
55. Keskitalo, J., Bergquist, G., Gardeström, P., and Jansson, S. (2005). A cellular timetable of autumn senescence. Plant Physiol. *139*, 1635–1648.
56. Inouye, D.W. (2008). Effects of climate change on phenology, frost damage, and floral abundance of montane wildflowers. Ecology *89*, 353–362.
57. Liu, Q., Piao, S., Janssens, I.A., Fu, Y., Peng, S., Lian, X., Ciais, P., Myneni, R.B., Peñuelas, J., and Wang, T. (2018). Extension of the growing season increases vegetation exposure to frost. Nat. Commun. *9*, 426.
58. White, M.A., de Beurs, K.M., Didan, K., Inouye, D.W., Richardson, A.D., Jensen, O.P., O'Keefe, J., Zhang, G., Nemani, R.R., van Leeuwen, W.J.D., et al. (2009). Intercomparison, interpretation, and assessment of spring phenology in North America estimated from remote sensing for 1982-2006. Glob. Chang. Biol. *15*, 2335–2359.
59. Keenan, T.F., Gray, J., Friedl, M.A., Toomey, M., Bohrer, G., Hollinger, D.Y., Munger, J.W., O'Keefe, J., Schmid, H.P., Wing, I.S., et al. (2014). Net carbon uptake has increased through warming-induced changes in temperate forest phenology. Nat. Clim. Chang. *4*, 598–604.
60. Piao, S., Ciais, P., Friedlingstein, P., Peylin, P., Reichstein, M., Luyssaert, S., Margolis, H., Fang, J., Barr, A., Chen, A., et al. (2008). Net carbon dioxide losses of northern ecosystems in response to autumn warming. Nature *451*, 49–52.
61. Seidl, R., Thom, D., Kautz, M., Martin-Benito, D., Peltoniemi, M., Vacchiano, G., Wild, J., Ascoli, D., Petr, M., Honkaniemi, J., et al. (2017). Forest disturbances under climate change. Nat. Clim. Chang. *7*, 395–402.
62. Hilker, T., Hall, F.G., Coops, N.C., Lyapustin, A., Wang, Y., Nesic, Z., Grant, N., Black, T.A., Wulder, M.A., Kljun, N., et al. (2010). Remote sensing of photosynthetic light-use efficiency across two forested biomes: Spatial scaling. Remote Sens. Environ. *114*, 2863–2874.
63. Filella, I., Penuelas, J., Llorens, L., and Estiarte, M. (2004). Reflectance assessment of seasonal and annual changes in biomass and CO2 uptake of a Mediterranean shrubland submitted to experimental warming and drought. Remote Sens. Environ. *90*, 308–318.
64. Yang, J., and Huang, X. (2021). The 30 m annual land cover dataset and its dynamics in China from 1990 to 2019. Earth Syst. Sci. Data *13*, 3907–3925.
65. Mu, H., Li, X., Wen, Y., Huang, J., Du, P., Su, W., Miao, S., and Geng, M. (2022). A global record of annual terrestrial Human Footprint dataset from 2000 to 2018. Sci. Data *9*, 176.
66. Nelson, A., Weiss, D.J., van Etten, J., Cattaneo, A., McMenomy, T.S., and Koo, J. (2019). A suite of global accessibility indicators. Sci. Data *6*, 266.
67. Jing, W., Yang, Y., Yue, X., and Zhao, X. (2016). A Spatial Downscaling Algorithm for Satellite-Based Precipitation over the Tibetan Plateau Based on NDVI, DEM, and Land Surface Temperature. Remote Sens *8*, 655.
68. Hengl, T., Mendes de Jesus, J., Heuvelink, G.B.M., Ruiperez Gonzalez, M., Kilibarda, M., Blagotić, A., Shangguan, W., Wright, M.N., Geng, X., Bauer-Marschallinger, B., et al. (2017). SoilGrids250m: Global gridded soil information based on machine learning. PLoS One *12*, e0169748.
69. Friedl, M., Gray, J., and Sulla-Menashe, D. (2022). MODIS/Terra+Aqua Land Cover Dynamics Yearly L3 Global 500m SIN Grid V061 (NASA EOSDIS Land Processes DAAC).
70. Wang, D. (2021). MODIS/Terra+Aqua Photosynthetically Active Radiation Daily/3-Hour L3 Global 1km SIN Grid V061 (NASA EOSDIS Land Processes DAAC).
71. Wan, Z., Hook, S., and Hulley, G. (2015). MODIS/Terra Land Surface Temperature/Emissivity 8-Day L3 Global 1km SIN Grid V061 (NASA EOSDIS Land Processes DAAC).
72. Shi Gaosong, L.I.Q.S.W. (2022). A 1 km Daily Soil Moisture Dataset over China Based on Situ Measurement (2000-2020).
73. Friedl, M., and Sulla-Menashe, D. (2022). MODIS/Terra+Aqua Land Cover Type Yearly L3 Global 500m SIN Grid V061 (NASA EOSDIS Land Processes Distributed Active Archive Center).
74. Ewers, R.M., and Rodrigues, A.S.L. (2008). Estimates of reserve effectiveness are confounded by leakage. Trends Ecol. Evol. *23*, 113–116.
75. Fuller, C., Ondei, S., Brook, B.W., and Buettel, J.C. (2019). First, do no harm: A systematic review of deforestation spillovers from protected areas. Glob. Ecol. Conserv. *18*, e00591.
76. Zhang, D., Wang, H., Wang, X., and Lü, Z. (2020). Accuracy assessment of the global forest watch tree cover 2000 in China. Int. J. Appl. Earth Obs. Geoinf. *87*, 102033.
77. Feng, C., Cao, M., Wang, W., Wang, H., Liu, F., Zhang, L., Du, J., Zhou, Y., Huang, W., and Li, J. (2021). Which management measures lead to better performance of China's protected areas in reducing forest loss? Sci. Total Environ. *764*, 142895.
78. Ribas, L.G.d.S., Pressey, R.L., Loyola, R., and Bini, L.M. (2020). A global comparative analysis of impact evaluation methods in estimating the effectiveness of protected areas. Biol. Conserv. *246*, 108595.
79. Schleicher, J., Eklund, J., D Barnes, M., Geldmann, J., Oldekop, J.A., and Jones, J.P.G. (2020). Statistical matching for conservation science. Conserv. Biol. *34*, 538–549.
80. Joppa, L.N., and Pfaff, A. (2009). High and Far: Biases in the Location of Protected Areas. PLoS One *4*, e8273.
81. Oldekop, J.A., Holmes, G., Harris, W.E., and Evans, K.L. (2016). A global assessment of the social and conservation outcomes of protected areas. Conserv. Biol. *30*, 133–141.
82. Ren, G., Young, S.S., Wang, L., Wang, W., Long, Y., Wu, R., Li, J., Zhu, J., and Yu, D.W. (2015). Effectiveness of China's National Forest Protection Program and nature reserves. Conserv. Biol. *29*, 1368–1377.
83. Sze, J.S., Carrasco, L.R., Childs, D., and Edwards, D.P. (2021). Reduced deforestation and degradation in Indigenous Lands pan-tropically. Nat. Sustain. *5*, 123–130.
84. Negret, P.J., Marco, M.D., Sonter, L.J., Rhodes, J., Possingham, H.P., and Maron, M. (2020). Effects of spatial autocorrelation and sampling design on estimates of protected area effectiveness. Conserv. Biol. *34*, 1452–1462.
85. Stuart, E.A. (2010). Matching Methods for Causal Inference: A Review and a Look Forward. Stat. Sci. *25*, 1–21.
86. Geldmann, J., Manica, A., Burgess, N.D., Coad, L., and Balmford, A. (2019). A global-level assessment of the effectiveness of protected areas at resisting anthropogenic pressures. Proc. Natl. Acad. Sci. USA *116*, 23209–23215.
87. Sekhon, J.S. (2011). Multivariate and Propensity Score Matching Software with Automated Balance Optimization: The Matching Package for R. J. Stat. Softw. *42*, 1–52.
88. Peng, D., Zhang, X., Wu, C., Huang, W., Gonsamo, A., Huete, A.R., Didan, K., Tan, B., Liu, X., and Zhang, B. (2017). Intercomparison and evaluation of spring phenology products using National Phenology Network and AmeriFlux observations in the contiguous United States. Agric. For. Meteorol. *242*, 33–46.
89. Wang, L., De Boeck, H.J., Chen, L., Song, C., Chen, Z., McNulty, S., and Zhang, Z. (2022). Urban warming increases the temperature sensitivity of spring vegetation phenology at 292 cities across China. Sci. Total Environ. *834*, 155154.
90. Zheng, Q., Teo, H.C., and Koh, L.P. (2021). Artificial Light at Night Advances Spring Phenology in the United States. Remote Sens *13*, 399.
91. Mann, H.B. (1945). NONPARAMETRIC TESTS AGAINST TREND. Econometrica *13*, 245–259.
92. Kendall, M.G. (1975). Rank Correlation Methods.
93. Liu, F., Feng, C., Zhou, Y., Zhang, L., Du, J., Huang, W., Luo, J., and Wang, W. (2022). Effectiveness of functional zones in National Nature Reserves for the protection of forest ecosystems in China. J. Environ. Manage. *308*, 114593.
94. Güçlü, Y.S. (2020). Improved visualization for trend analysis by comparing with classical Mann-Kendall test and ITA. JHyd *584*, 124674.
95. Zeng, Z., Wu, W., Ge, Q., Li, Z., Wang, X., Zhou, Y., Zhang, Z., Li, Y., Huang, H., Liu, G., and Peñuelas, J. (2021). Legacy effects of spring phenology on vegetation growth under preseason meteorological drought in the Northern Hemisphere. Agric. For. Meteorol. *310*, 108630.
96. Güsewell, S., Furrer, R., Gehrig, R., and Pietragalla, B. (2017). Changes in temperature sensitivity of spring phenology with recent climate warming in Switzerland are related to shifts of the preseason. Glob. Chang. Biol. *23*, 5189–5202.

STAR★METHODS

KEY RESOURCES TABLE

REAGENT or RESOURCE	SOURCE	IDENTIFIER
Deposited data		
China land cover datasets	Yang and Huang. 2021[64]	https://doi.org/10.5281/zenodo.4417810
Spatial distribution map of roads in China	Resource and Environment Science and Data Center	https://www.resdc.cn
DEM data	Shuttle Radar Topography Mission	https://www.usgs.gov
Global record of annual terrestrial Human Footprint dataset	Mu et al. 2022[65]	https://doi.org/10.6084/m9.figshare.16571064
Map of travel time to cities and ports in the year 2015	Nelson et al. 2019[66]	https://figshare.com/articles/dataset/Travel_time_to_cities_and_ports_in_the_year_2015/7638134/4
Monthly near-surface mean air temperature dataset at 1km resolution for China region	Jing et al. 2016[67]	http://www.geodata.cn/data/datadetails.html?dataguid = 3034046&docId = 6620
Monthly Precipitation Dataset at 1km Resolution for China Region	Jing et al. 2016[67]	http://www.geodata.cn/data/datadetails.html?dataguid = 2329433&docId = 6502
Relative humidity	Jing et al. 2016[67]	http://www.geodata.cn/data/datadetails.html?dataguid = 5361255&docId = 6503
Global gridded soil information map	Hengl et al. 2017[68]	https://maps.isric.org
Moderate Resolution Imaging Spectroradiometer (MODIS) Land Cover Dynamics (MCD12Q2) Version 6.1 data	Friedl et al. 2022[69]	https://lpdaac.usgs.gov/products/mcd12q2v061
Photosynthetically Active Radiation (PAR) gridded Level 3 product combined by Moderate Resolution Imaging Spectroradiometer (MODIS) Terra and Aqua	Wang et al. 2021[70]	https://lpdaac.usgs.gov/products/mcd18a2v061
Terra Moderate Resolution Imaging Spectroradiometer (MODIS) Land Surface Temperature/Emissivity 8-Day (MOD11A2) Version 6.1 product	Wan et al. 2015[71]	https://lpdaac.usgs.gov/products/mod11a2v061
1 km daily soil moisture dataset over China	Shi et al. 2022[72]	https://data.tpdc.ac.cn/en/data/49b22de9-5d85-44f2-a7d5-a1ccd17086d2
Moderate Resolution Imaging Spectroradiometer (MODIS) Land Cover Type (MCD12Q1) Version 6.1 data product combined by the Terra and Aqua	Friedl et al. 2022[73]	https://lpdaac.usgs.gov/products/mcd12q1v061

RESOURCE AVAILABILITY

Lead contact

Further information and requests for resources and reagents should be directed to and will be fulfilled by the lead contact, Jun Ma (ma_jun@fudan.edu.cn).

Materials availability

This study did not generate new unique reagents.

Data and code availability

- All datasets used in this study are publicly available and can be accessed via the links provided in the key resources table.
- No customized codes are used in the study.
- Any additional information is available from the lead contact upon request

METHOD DETAILS

Selection of PAs

Based on the list of nature reserves from the Ministry of Ecology and Environment of the People's Republic of China (MEE), we take 257 national nature reserves established before 2000 with forests as the main ecosystem (forest area is more than 10 km^2) for our research area (Figure S1A; Table S1). These PAs cover temperate, subtropical, and tropical zones, spanning both marine and continental climates, with areas ranging from 13 km^2 to 151940 km^2 (Figure S2).

PAs' inside and outside gradients

We created a buffer belt with a distance of 30 km outside each PA. Considering the possible "leakage or spillover effect" of the adjacent areas outside PAs,[74,75] we excluded the 0–10 km area and reserved the remaining part as the corresponding unprotected part to each PA (Figure S1B).

We used 30 m resolution land use data of China land cover datasets (CLCD)[64] to identify the distribution of forests inside and outside of PAs. This product is a Landsat-based land cover dynamic dataset specially developed for the China region, and the accuracy has been verified by two open-source test sets and one visual interpretation test set. The dataset was aggregated to 500 m and then converted into a binary forest/non-forest map using the threshold of 20% forest tree cover.[76,77] To exclude the influence of forest cover change on the estimations of LSP indicators, we only focused on the forest region that did not change after 2000.

We adopted the propensity matching approach[78,79] to control for the differences inside and outside of each PA that may interfere with our assessment of the impact of PAs on forest vegetation phenology. This is necessary because PAs are not randomly located in the landscape but are often biased toward remote areas where the land value is low.[80] Specifically, for each forest pixel inside a PA, the matching method finds counterparts in the buffer zone that are similar in terms of 13 socioeconomic and biophysical attribute variables based on existing studies,[81–83] including tree cover, distance to the main road, elevation, slope, aspect, topographic position index, human footprint index, travel time to the nearest big city, precipitation, temperature, soil sand, silt, and clay content.

This matching method was performed based on a propensity score which measures the probability of a pixel being located inside a PA given its values on the 13 variables. The propensity score summarized the attribute variables into a single scalar variable[84,85] and was used to determine the similarity between each protected forest pixel and those in the buffer zone. To improve the matching quality, we used a 1:1 nearest neighbor match without replacement for all variables. The matching was done with the "linear-logit" method and the caliper size was 0.25.[86] This meant that protected forest pixels were only compared to unprotected forest pixels with the closest match for climate background, topography condition, and initial pressure. We performed the matching analyses in R software using the "Matching" package.[87]

Extraction of LSP indicators

We used the MODIS MCD12Q2 V6.1 land surface phenology dataset,[69] which provides information such as the range and sum of the enhanced vegetation index (EVI) calculated from the MODIS surface reflectance data of each pixel. The MODIS LSP product was derived from 16-day composites of NBAR EVI2 that are updated daily with a spatial resolution of 500 m, which has been widely used in the study of vegetation phenology.[88–90] In this product, the start of greenup, greenup midpoint, and maturity dates are retrieved as the first date within the greenup segment where the NBAR-EVI2 time series crosses 15, 50, and 90% of the greenup segment NBAR-EVI2 amplitude (peak NBAR-EVI2 - segment start EVI; Figure S4). Similarly, the start of senescence, senescence midpoint, and dormancy are retrieved as the last date within the greendown segment where the NBAR-EVI2 time series crosses 90, 50, and 15% of the greendown segment NBAR-EVI2 amplitude[69](peak NBAR-EVI2 – segment end NBAR-EVI2; Figure S4). To improve the accuracy of our analysis, we excluded all pixels with "poor quality" based on "QA_Detailed" files provided by the product. Then, we used the SDS names of the "Greenup" value as the start date of the season (SOS) and the "Dormancy" as the end date of the season (EOS), and the length of the season (LOS) was obtained by EOS minus SOS.

Climatic data

Since climatic conditions are the direct driver of variations in vegetation phenology, we selected some important microclimatic indicators closely related to vegetation growth to explore the possible reasons for the phenological differences between inside and outside PAs, including land surface temperature (LST), soil moisture (SM), relative humidity (RH), and photosynthetically active radiation (PAR). To improve the accuracy of our analysis, we only extracted LST with estimated emissivity error $\leq$0.02 and LST error $\leq$2 K. The nearest neighbor interpolation method was used to interpolate all the climate and elevation raster data to the size of 500 m to match the phenological remote sensing data.

Quantifying differences in indicators inside and outside protected areas

We used the average of the pixels of remote sensing data inside and outside the protected areas to represent the average within each area, respectively. The phenological differences between inside and outside PA were defined as $\Delta SOS = SOS_{inside} - SOS_{outside}$, $\Delta EOS = EOS_{inside} - EOS_{outside}$, and $\Delta LOS = LOS_{inside} - LOS_{outside}$. The microclimatic differences were defined as follows: ΔLST_day, daytime LST difference; ΔLST_night, night-time LST difference; ΔSM, soil moisture difference; ΔRH, relative humidity difference; ΔPAR, photosynthetically active radiation difference.

The spatial distributions of the phenological differences between inside and outside PAs (i.e., ΔSOS, ΔEOS, and ΔLOS) from 2018 to 2020 (mean values of 3 years) based on nationwide scale and latitude were then analyzed.

Classification of protected areas

Due to the large spatial span of our protected area, including different forest types. Therefore, we used the product of MCD12Q1[73] to classify protected areas here. If the coverage rate of a certain type of forest in the protected area exceeded 60%, it would be classified as the corresponding forest type. Finally, the protected areas were divided into five categories (Figure S3; Table S1): EBF, evergreen broadleaf forests; ENF, evergreen needleleaf forests; DBF, deciduous broadleaf forests; DNF, deciduous needleleaf forests; MF, mixed forests. Since only two protected areas belong to the DNF type, such an insufficient sample size is not conducive to our analysis, we have excluded these types of protected areas in subsequent analysis of forest types.

QUANTIFICATION AND STATISTICAL ANALYSIS

We used the Wilcoxon signed rank test to determine whether there were significant differences in LSP indicators between inside and outside PAs.

Linear regression analysis was used to investigate the trends in the distribution of phenological differences inside and outside with latitude.

We applied the Mann–Kendall trend test to investigate the trend of the phenological difference. Mann–Kendall is a non-parametric statistical approach widely used to assess the significance of a trend,[91–94] in which $|Z| \geq 1.96$ indicates the results pass the 95% confidence test and show a significant trend of change. On the contrary, it is not significant.

To determine the main controlling factors for the phenological differences, we conducted Spearman partial correlation analysis (two-tailed) between the phenological differences and the latitude, longitude, established year, annual mean temperature, annual precipitation of PAs, and microclimatic differences. Because the occurrence of phenological events has the greatest correlation with the preseason climate conditions,[95,96] we used the corresponding preseason climate data based on characteristics of phenological data. The mean values of microclimatic data from March to May were corresponding to SOS, and mean values from September to November were corresponding to EOS, while mean annual values were corresponding to LOS.

While controlling other factors, we determined the partial correlation of each factor, in which the size of the partial correlation coefficient reflects the influence of the independent variable on the dependent variable. We further used linear regression to explore the relationship of the phenological differences with ΔLST_day and ΔLST_night respectively. The R-squared value was used to evaluate the strength of the linear correlation, and the significance of the equation was tested. Furthermore, we conducted a forward stepwise linear regression analysis and established an equation between the phenological differences and the microclimatic differences. In each step, an explanatory variable was considered to either add or subtract from the set of variables based on a sequence of F tests. By comparing the significance and R-squared value of different equations, we selected the optimal model to characterize the impact mechanism of phenological difference.

The significance level of this study was 0.05. All data analysis and mapping were completed in R-4.3.1 software and ArcGIS-10.8 software.